

Infra-Red Study of Surface Carbonation on Polycrystalline Magnesium Hydroxide

Heekyoung Kwon and Dong Gon Park*

Department of Chemistry, Sookmyung Women's University, Seoul 140-742, Korea. *E-mail: dgpark@sm.ac.kr

Received July 27, 2009, Accepted September 9, 2009

Carbonation of $\text{Mg}(\text{OH})_2$ at 300 °C was studied by Infrared spectroscopy. Dehydroxylation and carbonation reactions were carried out in consecutive manner *via* 2-step procedure. Unidentate carbonates were produced only on defective surface of MgO in situ generated by dehydroxylation of $\text{Mg}(\text{OH})_2$ under dynamic vacuum. Bicarbonates and bidentate carbonates were not observed. Generation of unidentate carbonates was accompanied by decrease of 1-coordinated hydroxides and concomitant increase of multi-coordinated hydroxides on the surface. Postulated reaction mechanism for the carbonation of $\text{Mg}(\text{OH})_2$ at 300 °C was proposed.

Key Words: Carbonation, Dehydroxylation, Carbonates, Hydroxides

Introduction

Much effort is being made to devise effective ways to remove atmospheric CO_2 , and to store it for extended time.¹ Several approaches for the CO_2 -sequestration include transformation of CO_2 into carbonate minerals.² The most viable candidates for the carbonate mineralization are oxides or hydroxides of Mg or Ca. They generate stable carbonates which are insoluble in water. A major obstacle in applying them for CO_2 -sequestration is that the rate of carbonation is very low. Challenge is to find a practical way to enhance the carbonation process. For the purpose, it is required to expand understanding on the carbonation process of these materials.

Studies on $\text{Mg}(\text{OH})_2$ show that the carbonation process is quite complex, that exact mechanism cannot easily be clarified.^{3,4} Carbonation was carried out at the temperature higher than 300 °C, where reasonable conversion to MgCO_3 could be reached. Apparently, many different reactions were concurrently involved with the generation of MgCO_3 at the temperature range. Not only carbonation, but dehydroxylation of $\text{Mg}(\text{OH})_2$ into MgO proceeded simultaneously. As reaction temperature was raised above 400 °C, decarbonation also started to occur, competing with the simultaneous dehydroxylation and carbonation. Generation of MgCO_3 layer also retarded further carbonation by pacifying surface of the solid sample. Further complicating the studies on the kinetics and mechanisms, dehydroxylation accompanied morphological reconstruction, as well as in situ generation of MgO phase.⁵⁻⁷ Therefore, fundamental understanding of the oxide surfaces is also necessary to fully describe carbonation of $\text{Mg}(\text{OH})_2$. Surfaces of metal oxides play an important role in various solid-gas reactions occurring in nature or in industrial processes, such as catalysis, corrosion, and many geological processes.⁸

In this report, conversion of $\text{Mg}(\text{OH})_2$ into MgCO_3 was carried out *via* 2-step reactions at low temperature of 300 °C, and reactions occurring on the solid surface were investigated by Fourier transformed infrared (FTIR) spectroscopy.

Experimentals

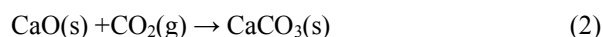
$\text{Mg}(\text{OH})_2$ was prepared by hydration of commercial MgO (99%, 325 mesh) purchased from Sigma-Aldrich. In 1-L round bottom flask equipped with a water condenser, 20 g of MgO was dispersed in 500 mL distilled water. The mixture was refluxed for 24 h. The white paste obtained by filtration was dried in oven at 120 °C overnight. Fine white powder of $\text{Mg}(\text{OH})_2$ was obtained after brief grinding by agate mortar and pestle.

Pre-treatment and carbonation reaction were carried out in 100 mL Schlenk reaction vessel (SRV) attached to double manifold inert-atmosphere system. The manifold for inert gas was modified so that Ar, CO_2 , or dynamic vacuum could be switched at will, without any interruption during heat treatment. In the 100 mL SRV, 3.0 g of $\text{Mg}(\text{OH})_2$ powder was loaded, then was heated at 300 °C (or 500 °C) by using the home-made heater. The flow rate of the gas was 33 mL/min.

FTIR spectrum was taken by JASCO 670 FTIR spectrometer from powder sample pelletized with KBr. Powder sample in SRV was taken out and made into pellet under Ar atmosphere in VAC glove box. The KBr pellet was made by using small bolt-type pellet presser purchased from Sigma-Aldrich, and kept as standing in the bolt under dry Ar all the time, thereby eliminating contact with atmospheric CO_2 or moisture. Powder X-ray diffraction pattern was taken with AXS-D8 ADVANCE diffractometer from Bruker. By using modified sample holder covered by Mylar film, contact with atmospheric CO_2 or moisture was eliminated. BET surface area was measured by GEMINI V from Micromeritics.

Results and Discussion

Mg and Ca are abundant elements on earth, and their oxides and hydroxides are relatively cheap and readily available. The capture of CO_2 by these oxides or hydroxides may occur by one of following reactions.



Carbonation in practice is carried out in dynamic flow of reactant gases, which is non-equilibrium condition. In such dynamic system, the partial pressure of gas product never reaches standard state of 1 atm. Therefore, thermodynamic parameters in the Table 1 do not exactly reflect the real conditions. Still, thermodynamic parameters tabulated for the standard state in equilibrium may provide instructive insight on the consequences from raising temperature in the real situation.

A brief calculation of a few basic thermodynamic parameters (provided in Table 1) suggests that Ca minerals may be better candidates for locking off CO₂ into carbonate minerals than Mg. Carbonation of Ca minerals is strongly inclined toward forward reaction (large negative values of $\Delta G^\circ_{\text{reaction}}$). Historical human experience already demonstrated this aspect, by Romans heavily using slaked lime [Ca(OH)₂] as mortar in construction. Buildings and aqueducts whose bricks were glued together with CaCO₃, in situ generated from the Ca(OH)₂ used, are still standing after several hundred years. But, for some technical purposes, one might need to reverse the carbonation reaction at will, to release CO₂ at some point, thereby refreshing sequestering reagents for recycle. For such specific purpose, Mg minerals could be better candidates than Ca.

In any case, rate for carbonation at ambient temperature is too slow to be practical. From previous studies by others, it was demonstrated that the temperature had to be raised, in order to accomplish carbonation in practical rate, by providing activation energy to overcome kinetic barrier.^{3,4} But, the kinetic enhancement starts to come into conflict with thermodynamics in the carbonation of these minerals. Even though all four reactions above are spontaneous at room temperature (minus value of $\Delta G^\circ_{\text{reaction}}$ in Table 1), calculation on reversal temperature in Table 1 suggests the carbonation should become unfavorable as temperature goes up. The extent of offset paid by enhancing the reaction rate by raising temperature would be especially problematic for MgO being the one most signi-

Table 1. Standard molar free energy of reaction ($\Delta G^\circ_{\text{reaction}}$) calculated from tabulated values of standard molar enthalpy of formation (ΔH°_f) and standard molar entropy (S°). Equilibrium was assumed where the pressures of all the gases are 1 atm (standard state). Calculation was made to get a rough idea on the consequences of raising reaction temperature.

Reaction No.	$\Delta G^\circ_{\text{reaction}}$ (KJ/mol) at 25 °C	T for $\Delta G^\circ_{\text{reaction}} = 0$ (°C)*
(1)	-45.2	267
(2)	-134.7	928
(3)	-12.9	598
(4)	-65.7	3961

*Calculated from $\Delta G^\circ_{\text{reaction}} = (\Delta H^\circ_{\text{reaction}}) - T(\Delta S^\circ_{\text{reaction}})$.

Table 2. Descriptions of the 2-step reactions carried out for Mg(OH)₂. Surface area was measured by BET method.

Sample	pre-treatment at 300 °C* (1st step)	carbonation at 300 °C* (2nd step)	Surface area m ² /g
Mg(OH) ₂	no	no	28
M300C	no	6 h/1 atm CO ₂	59
M300AC	19 h/1 atm Ar	12 h/1 atm CO ₂	46
M300V	19 h/10 ⁻³ torr	no	263
M300VC	19 h/10 ⁻³ torr	6 h/1 atm CO ₂	-
M500VC	19 h/10 ⁻³ torr at 500 °C	6 h/1 atm CO ₂ at 300 °C	268

*The flow rate of the gas was 33 mL/min.

ficantly influenced. Low conversion may be unavoidable in the carbonation of MgO as reaction temperature goes up. This conflicting aspect is apparent in previous studies. Study on Mg(OH)₂ by others verified that dehydroxylation and carbonation reactions occurred simultaneously, and conversion to MgCO₃ was about 15% at best.^{3,4} That maximum conversion was only possible between 300 - 500 °C, where the rate of dehydroxylation of Mg(OH)₂ into MgO was substantial. At the temperature range, it was observed that decarbonation (reverse reaction) already started to occur.³ It was also suggested that the generation of MgCO₃ layers on the surface impeded further carbonation. It was not obvious whether the carbonation was occurring on MgO or Mg(OH)₂, because the reaction mechanism was not clearly elucidated.

In an effort to make separate observations on dehydroxylation and carbonation, which normally proceed simultaneously, carbonation on Mg(OH)₂ was carried out *via* 2-step reactions at 300 °C. Conversion to MgCO₃ was known to be low at the temperature.³ The rate of dehydroxylation of Mg(OH)₂ is also very low at 300 °C. But, it can be accelerated by lowering the activation energy by carrying out dehydroxylation in dynamic vacuum. It is reported that the apparent activation energies for dehydroxylation of Mg(OH)₂ increase as following order; in vacuum (53 - 126 KJ/mol)⁹ < in helium (146 KJ/mol)³ < in CO₂ (304 KJ/mol)³. It is also known that the apparent activation energy of the dehydroxylation increases with partial pressure of H₂O.¹⁰ By cutting off the supply of CO₂ and lowering the activation energy, only dehydroxylation reaction could be carried out in the first step (pre-treatment in Table 2). In second step, pure CO₂ at 1 atm was flushed over the sample, thereby discouraging dehydroxylation by raising the activation energy, at the same time encouraging carbonation reaction by supplying reactant. In this consecutive manner, dehydroxylation and carbonation reactions could be carried out separately. Thereby, complication coming from simultaneous reactions could be minimized during observation.

Table 2 provides a list of several different pre-treatments on Mg(OH)₂ samples, prior to the carbonation in pure CO₂ atmosphere. Carbonation (2nd step reaction) was carried out immediately after the pre-treatment (1st step reaction), by directly exchanging the gas atmosphere without any interruption or cooling. For all but one case, both pre-treatment and carbona-

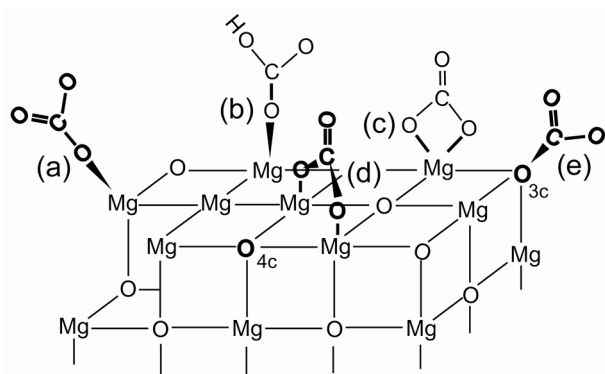


Figure 1. Schematic representations of different conformations of carbonates on the surface of MgO. (a) unidentate carbonate, (b) bicarbonate, (c) bidentate carbonate, (d) bridging carbonate, and (e) multi-coordinated carbonate ($O_{3c}-CO_2$).

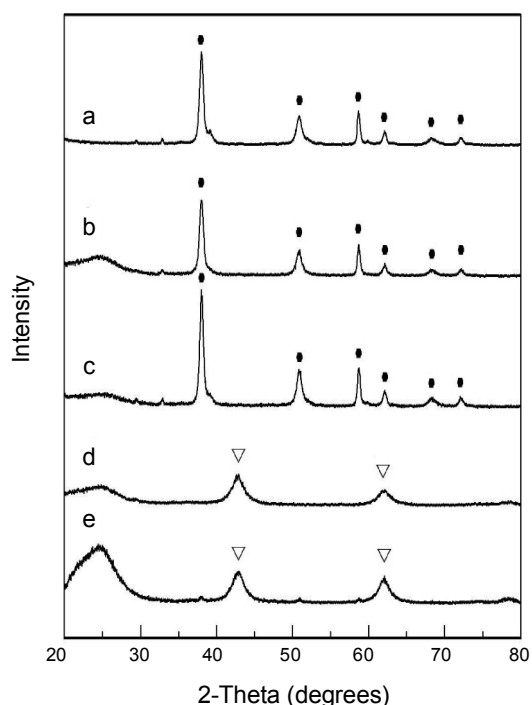


Figure 2. Powder X-ray diffraction patterns obtained after carrying out the reactions described in Table 2. (a) $Mg(OH)_2$ as prepared by hydration of commercially obtained MgO, (b) exposed to CO_2 at 300 °C without any pre-treatment (M300C), (c) exposed to CO_2 after pre-treatment in Ar, at 300 °C (M300AC), (d) after pre-treatment at 300 °C under dynamic vacuum (M300V), (e) exposed to CO_2 after pre-treatment under dynamic vacuum, at 300 °C (M300VC). Closed circles (●) and open triangles (▽) designate diffraction peaks from $Mg(OH)_2$ and MgO, respectively.

tion reaction were carried out at 300 °C. In order to eliminate 1-coordinated hydroxides on the surface, one specific sample (M500VC) was pre-treated at 500 °C, and cooled down to 300 °C where subsequent carbonation was carried out.

In general, observed features in a solid-gas reaction are strongly related to the characteristics of the solid surface, rather than its bulk. Whereas X-ray diffraction pattern provides features mostly from bulk, FTIR spectrum gives valuable in-

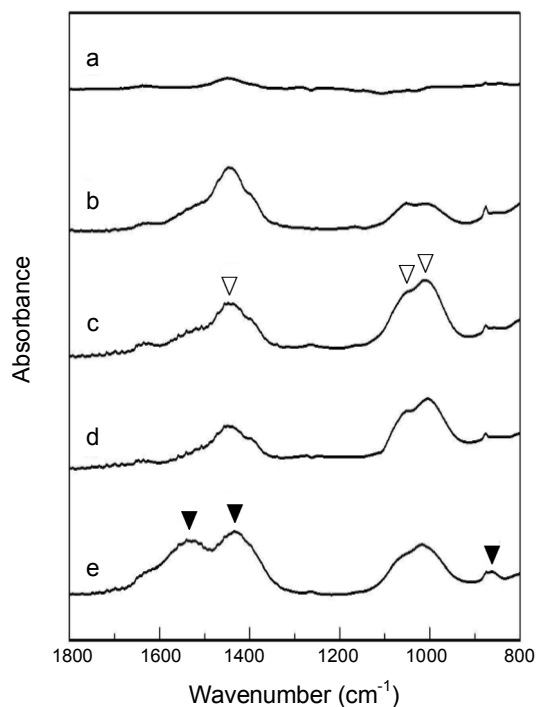


Figure 3. FTIR spectra taken from samples pelletized with KBr, after carrying out the reactions described in Table 2. (a) $Mg(OH)_2$ as prepared, (b) M300C, (c) M300AC, (d) M300V, and (e) M300VC. Open triangles (▽) and closed triangles (▼) designate MgO and $MgCO_3$, respectively.

formation on the surface of solids. As for the surface carbonates, the assignments of the vibrational frequencies are relatively well documented.¹¹⁻¹⁶ Graphic representations for different carbonates attainable on the surface of MgO are shown in Figure 1. Four major vibrational frequencies for unidentate carbonates (Figure 1a) are assigned at 1510 - 1550, 1390 - 1410, 1035 - 1050, and 860 - 865 cm^{-1} .¹¹⁻¹³ Vibrational frequencies for bicarbonates (figure 1b) are assigned at 1655 - 1658, 1405 - 1419, and 1220 - 1223 cm^{-1} .^{11,13-15} Bidentate carbonates (Figure 1c) show peaks at 1665 - 1670, 1325 - 1330, 1005 - 1030, and 850 - 855 cm^{-1} .¹¹⁻¹³ Key signature of unidentate carbonate, distinguishing it from others, is separation between two major peaks which is 100 cm^{-1} .¹¹ Bridging carbonates (Figure 1d) and multi-coordinated carbonates (Figure 1e) have been seldom observed in any precedent reports on MgO. Only a theoretical calculation was carried out for multi-coordinated carbonate, $[O_{4c}-CO_2]^{2-}$, and vibrational frequencies were predicted at 1460, 1042, 945, and 794 cm^{-1} .¹⁶

Powder X-ray diffraction patterns and FTIR spectra obtained from the solid samples listed in Table 2 are shown in Figure 2 and Figure 3, respectively. After heating $Mg(OH)_2$ at 300 °C in pure CO_2 atmosphere without any pre-treatment, no apparent change is observed in the powder X-ray diffraction patterns (Figure 2a and 2b). FTIR spectra (Figure 3a and 3b) show several peaks developed after heating, in very weak intensity, at 1655, 1450, 1065, 1010, and 880 cm^{-1} . They were observed regardless of the CO_2 introduction (see Figure 3d), thereby excluding possibility of being surface carbonates. They became more prominent as heating lasts, and apparently

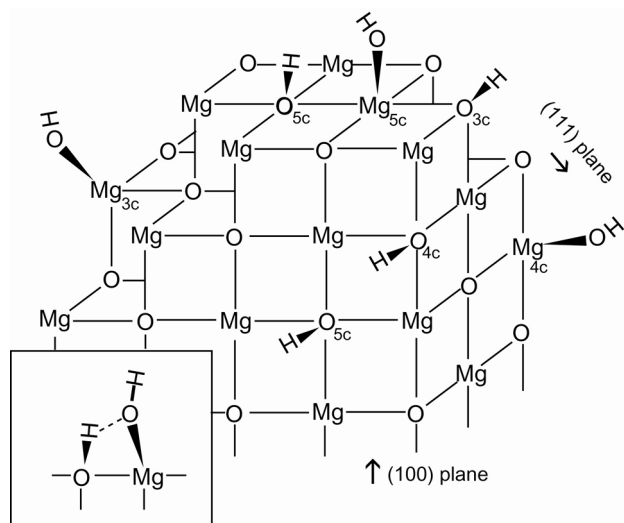


Figure 4. Schematic representation of defective surface of MgO. Diagram shows different kinds of surface hydroxides. Hydrogen bonding interaction between 1-coordinated hydroxide (proton acceptor) and multi-coordinated hydroxide (proton donor) is shown in the inset of the diagram.

were not related to major peaks around 3700 cm^{-1} in relative intensities. In previous studies on CP-MgO, these peaks were observed from MgO samples obtained by dehydration of $\text{Mg}(\text{OH})_2$.¹⁷ Therefore, these peaks were tentatively assigned to MgO phase on the surface generated by dehydration. It suggests that some $\text{Mg}(\text{OH})_2$ on the surface turned into MgO, but intensity from MgO was very weak. Dehydroxylation reaction was not significant at the temperature, and no carbonation product was observed. Likewise, no apparent change is observable in the powder X-ray diffraction patterns (Figure 2a and 2c) with the pre-treatment in Ar atmosphere. Very weak vibrational peaks from MgO can be located in Figure 3c, when the sample was pre-treated in Ar, indicating generation of a small fraction of MgO phase only on the surface. But, still no carbonate is observed, even after 19 h contact with pure CO_2 at $300\text{ }^\circ\text{C}$. These observations suggest that $\text{Mg}(\text{OH})_2$ as prepared does not react with CO_2 (pure/1 atm) at $300\text{ }^\circ\text{C}$, even with a small fraction of MgO layer on the surface. This outcome is consistent to the gravimetric analysis by others on $\text{Mg}(\text{OH})_2$,³ that exhibited the extents of both dehydroxylation and carbonation reactions were negligible at $300\text{ }^\circ\text{C}$.

MgO phase on the surface (dehydroxylation product), which inherently contains high concentration of defective sites, and is more reactive than MgO as bulk, must be playing an important role in the generation of MgCO_3 . It has been known that MgO with high concentration of defects on the surface exhibited unusually high reactivity toward many different chemicals.^{13,18,19} Such high surface-reactivity was found in MgO samples obtained by dehydrating $\text{Mg}(\text{OH})_2$ in non-equilibrium condition, such as under fast flow of dry gas, or under dynamic vacuum. Figure 2d and figure 3d show power X-ray diffraction pattern and FTIR spectrum of $\text{Mg}(\text{OH})_2$ heat treated at $300\text{ }^\circ\text{C}$ under dynamic vacuum for 19 h, respectively. Whereas dehydroxylation did not proceed deep into bulk in Ar or CO_2 atmosphere, it turned most of $\text{Mg}(\text{OH})_2$ into MgO under dynamic

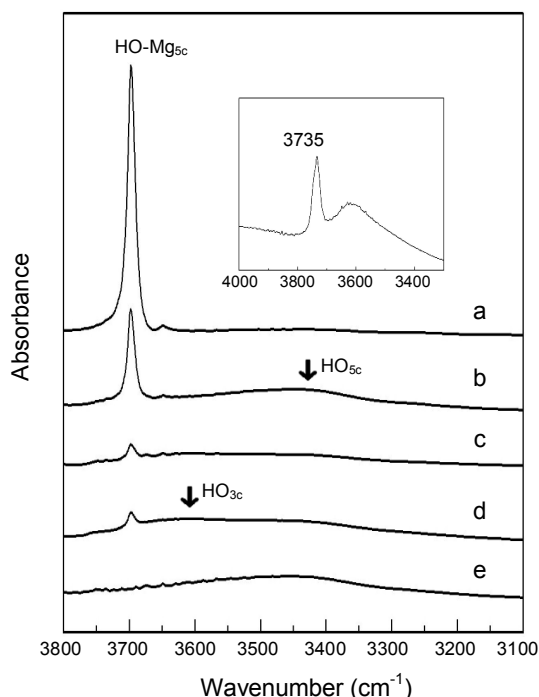


Figure 5. FTIR spectra taken from the samples exposed to CO_2 at $300\text{ }^\circ\text{C}$ for different duration. CO_2 gas was introduced immediately after 19 h pre-treatment under dynamic vacuum. (a) not exposed to CO_2 , only pre-treatment was carried out, (b) 6 h exposure, (c) 12 h exposure, and (d) 18 h exposure. Pre-treatment for (a) to (d) was carried out at $300\text{ }^\circ\text{C}$. Spectrum (e) was taken after pre-treatment at $500\text{ }^\circ\text{C}$, not exposed to CO_2 . The FTIR spectrum in the inset was taken from AP-MgO, obtained by pre-treating AP- $\text{Mg}(\text{OH})_2$ at $300\text{ }^\circ\text{C}$ under dynamic vacuum for 19 h. AP- $\text{Mg}(\text{OH})_2$ was synthesized by sol-gel/hyper critical drying.

vacuum, as can be seen in Figure 2d. Broadness of the diffraction peaks from MgO indicates the crystalline domain is in nano-scale, which is calculated by Scherrer equation to be 9 nm. BET surface area increased more than 5-fold ($263\text{ m}^2/\text{g}$), compared to $\text{Mg}(\text{OH})_2$ heat-treated under 1 atm. These characteristic changes allude to the generation of highly reactive defective sites on the surface of MgO.^{13,18,19} When CO_2 was introduced after the pre-treatment under dynamic vacuum, generation of surface carbonates was observed. FTIR spectrum in Figure 3e shows vibrational peaks at 1533 , 1430 , and 862 cm^{-1} , which can be assigned to unidentate carbonates bonded to Mg on the surface.¹¹⁻¹³ Remaining peak around 1050 cm^{-1} is obscured by overlapping MgO peaks. No peak was observed which could be assigned to bicarbonates or bidentate carbonates on the surface. Powder X-ray diffraction pattern in Figure 2e shows no peak related to MgCO_3 , indicating those unidentate carbonates were generated only on the surface. These observations from the 2-step reactions show that dehydroxylation process plays a critical role in the carbonation of $\text{Mg}(\text{OH})_2$, via providing reactive surfaces of MgO.

There can be many different hydroxyl groups on the surface of MgO. Depending on the coordination environments around Mg, where the hydroxide is bonded to, 1-coordinated hydroxides (referred as 'type A' by others)²⁰⁻²² can be designated as

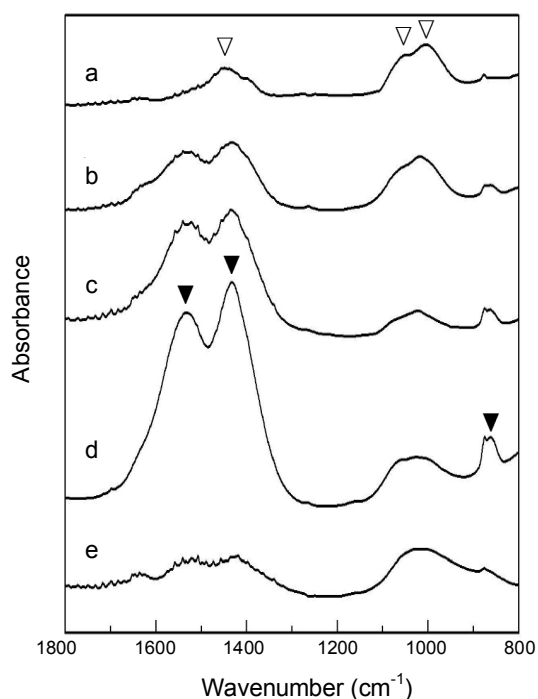


Figure 6. FTIR spectra taken from the samples exposed to CO₂ at 300 °C for different duration. CO₂ gas was introduced immediately after 19 h pre-treatment under dynamic vacuum. (a) not exposed to CO₂, only pre-treatment was carried out, (b) 6 h exposure, (c) 12 h exposure, and (d) 18 h exposure. Pre-treatment for (a) to (d) was carried out at 300 °C. Pre-treatment for (e) was carried out at 500 °C, and subsequently exposed to CO₂ for 12 h at 300 °C. Open triangles (∇) and closed triangles (▼) designate MgO and MgCO₃, respectively.

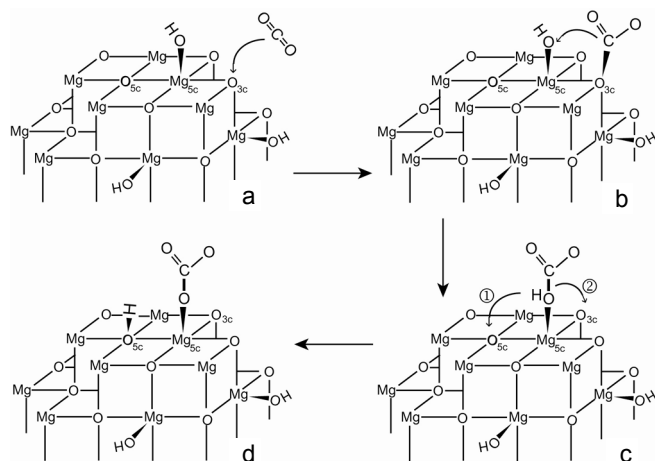
HO-Mg_{3c}, HO-Mg_{4c}, or HO-Mg_{5c}. Depending on the coordination environments around lattice O where H is bonded to, multi-coordinated hydroxides (referred as 'type B' by others)²⁰⁻²² can be designated as HO_{3c}, HO_{4c}, or HO_{5c}. As illustrated in Figure 4, Mg_{3c} and O_{3c} correspond to the atoms at the corners along high index plane [(111) for example] of MgO lattice. Mg_{4c} and O_{4c} are sitting along the edges. Mg_{5c} and O_{5c} are the ones embedded on (100) planes. In hydrogen bonding interaction among these surface hydroxides, multi-coordinated hydroxides behave as hydrogen donor, whereas 1-coordinated hydroxides act as hydrogen acceptor through oxygen.²² This hydrogen bonding interaction is schematically demonstrated in the inset of the Figure 4. Hydrogen bonding interaction with the lattice oxygen is also considered to exist, especially for the sample heat treated at high temperature above 500 °C.²² Vibrational peaks from multi-coordinated hydroxides get broad, because of these hydrogen bonding interactions. It was reported that peaks shift to lower frequency as number of coordination increases.^{23,24} Therefore, 1-coordinated hydroxides on the surface (proton acceptor) register relatively sharp peaks at high frequency region around 3700 cm⁻¹, whereas multi-coordinated hydroxides (proton donor) on the surface give broad featureless peaks around 3350 - 3650 cm⁻¹.²⁰⁻²⁴

Extensive studies have been carried out on the assignments of vibrational frequencies for these surface hydroxyl groups by others.²⁰⁻²⁸ Bonding in MgO is known to be highly cova-

lent. Not only inductive effect of highly electronegative oxygen, but also electron donating effect by lone pairs of oxygen has to be counted together in assessing the relative comparison of electron density for O-H bonding. Due to these two conflicting factors, some of these reports contain a few contradictory predictions, especially on the assignments on 'type A' hydroxides.^{22,23,24,28} Results of the ab initio calculation on MgO clusters show the Mg-OH bond length of 1-coordinated hydroxides increases as coordination number of Mg increases.²² The prediction made by the calculation also indicates the vibrational frequency of 1-coordinated hydroxides shifts to lower frequency as the coordination number of Mg increases. This prediction suggests the peak for HO-Mg_{5c} will be at lower frequency region compared to HO-Mg_{3c}.

After dehydroxylation under dynamic vacuum at 300 °C, duration of subsequent CO₂ contact was extended, and FTIR spectra were taken every 6 h. FTIR spectra in Figure 5 and Figure 6 show the spectral regions for surface hydroxides and for surface carbonates, respectively. The featureless broad peaks spanning from 3300 to 3650 cm⁻¹ in Figure 5 are assigned to multi-coordinated hydroxides (type B). The peak at 3697 cm⁻¹ is assigned to 1-coordinated hydroxides (type A) on the surface of MgO.²⁰⁻²⁸ The peak at 3697 cm⁻¹ was observed at lower frequency in 'type A' region. Therefore, coordination environment around Mg is tentatively assigned to be HO-Mg_{5c}. In order to get an additional physical evidence on this speculation, comparison was made by preparing AP-MgO *via* sol-gel/hyper-critical drying.^{13,18,19} It is known that AP-MgO contains large fraction of high index planes, thereby, high concentration of low coordination sites, such as corners (Mg_{3c} and O_{3c}) and edges (Mg_{4c} and O_{4c}). Vibrational spectrum taken from this highly defective AP-MgO was provided in the inset as comparison. The peak for the 1-coordinated hydroxides was observed at 3735 cm⁻¹, higher frequency than the one observed in the MgO generated by dehydroxylation of Mg(OH)₂. The broad peak for the multi-coordinated hydroxide is also observed as shifted to higher frequency region around 3600 cm⁻¹. Considering AP-MgO contains significantly higher proportion of low coordination sites than other MgO, those peaks observed at higher frequencies are tentatively assigned to HO-Mg_{3c} and HO_{3c}-. These observations corroborate the assignment of HO-Mg_{5c} to the peak at 3697 cm⁻¹, also conforming to the ab initio calculation by others.

In Figure 6, the increase of the peak intensity for the unidentate carbonates at 1533, 1430, and 862 cm⁻¹ is evident with extended duration of CO₂ exposure. No peak assignable to bi-carbonates or bidentate carbonates developed. It is interesting to note that the intensity of the hydroxide peak at 3697 cm⁻¹ in figure 5 decreases concomitantly with the increase of those carbonate peaks (comparing Figure 5 and Figure 6). Apparently, generation of surface carbonates accompanied disappearance of 1-coordinated hydroxides on the surface. It is obvious that 1-coordinated hydroxides on the surface of MgO are reactant, rather than being by-stander. Careful observation of Figure 5 also exhibited that a featureless broad peak developed around 3450 cm⁻¹ during initial 6 h period (Figure 5b), which was followed by another development of a broad peak around 3600 cm⁻¹ (Figure 5c and 5d). The broad featureless peaks around



Scheme I. Postulated reaction mechanism of the surface carbonation of $\text{Mg}(\text{OH})_2$.

3450 and 3600 cm^{-1} correspond to HO_{5c} and HO_{3c} , respectively. Therefore, generation of unidentate carbonate on the surface of MgO accompanied concurrent demise of 1-coordinated hydroxides, and the development of multi-coordinated hydroxides, as well.

In order to see whether the involvement of 1-coordinated hydroxides is necessary for the carbonation, they were intentionally eliminated by pre-treating $\text{Mg}(\text{OH})_2$ at $500\text{ }^\circ\text{C}$ (instead of $300\text{ }^\circ\text{C}$) under dynamic vacuum (sample M500VC). FTIR spectrum taken after pre-treatment at $500\text{ }^\circ\text{C}$ (Figure 5e) shows no prominent peak around 3700 cm^{-1} , suggesting that the 1-coordinated hydroxides were not present on the surface. After the pre-treatment at $500\text{ }^\circ\text{C}$, the sample was exposed to pure CO_2 at $300\text{ }^\circ\text{C}$ during 12 h, and not much carbonation occurred as can be seen in Figure 6e.

From these observations, we postulated possible mechanisms of the carbonation reactions at $300\text{ }^\circ\text{C}$, occurring on the reactive MgO surface generated by dehydroxylation of $\text{Mg}(\text{OH})_2$, and schematically proposed them in Scheme I. After dehydroxylation at $300\text{ }^\circ\text{C}$ under dynamic vacuum, MgO surfaces develop defective sites such as corners and edges. It was reported that the reactivity of defective sites increases as the coordination number decreases.^{13,18,19} Theoretical study by ab initio calculation also showed that CO_2 preferably chemisorbs on lower coordinated defective sites.¹⁶ Therefore, CO_2 adsorbs on highly reactive O_{3c} at the apex of the corners (scheme Ia and Ib). Then, CO_2 migrates to the adjacent 1-coordinated hydroxide, generating a protonated intermediate proposed in Scheme Ic. Subsequent deprotonation generates unidentate carbonate (Scheme Id). At the same time, protonation of lattice oxygen generates multi-coordinated hydroxide on the surface (Scheme Id). In early stage of the carbonation (initial 6 h), deprotonation proceeds along path ①, generating HO_{5c} . Later, it follows the path ②, generating HO_{3c} . The observations made on Figure 5 and Figure 6 conform to this proposed mechanism. As the outcome of these stepwise processes, the FTIR peak for the 1-coordinated hydroxide would shrink, and at the same time, the peaks for unidentate carbonates and multi-coordinated hydroxides should grow up.

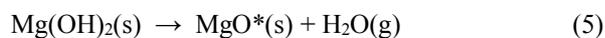
Theoretical calculation on MgO clusters suggested the chemisorption of CO_2 on defective sites was non-activated process, and generated multi-coordinated carbonates, without migration.¹⁶ Because the calculation was carried out on a cluster embedded in a large array of point charges (surrounding), possibility of the CO_2 migration was not counted in the theoretical study. Apparently, no such multi-coordinated carbonates were observed in our study, and only unidentate carbonate was generated. Also, it is interesting to note that bicarbonates would be produced if proton migrated to negatively charged end moiety of the carbonate. But, apparently it did not happen, and instead, the proton migrated opposite direction toward the surface, to combine with the multi-coordinated lattice oxygen.

Conclusion

By following 2-step procedure at $300\text{ }^\circ\text{C}$, dehydroxylation and carbonation reactions of $\text{Mg}(\text{OH})_2$ were carried out in consecutive manner, thereby trying to see the outcome of each reaction separately. It was shown that carbonation did not occur without preceding dehydroxylation of $\text{Mg}(\text{OH})_2$ into MgO . The carbonation product was obtained only on defective MgO surface, which was in situ generated by dehydroxylation of $\text{Mg}(\text{OH})_2$ under dynamic vacuum. The carbonation product was unidentate carbonates on the surface, and formation of bicarbonates and bidentate carbonates were not observed.

The generation of unidentate carbonates accompanied concurrent demise of 1-coordinated hydroxides on the surface of the defective MgO . Without 1-coordinated hydroxides on the surface, carbonates were not produced at $300\text{ }^\circ\text{C}$. As carbonation reaction proceeded, population of multi-coordinated hydroxides also increased.

On the basis of the observations made during 2-step reactions, postulated reaction mechanism was proposed for the carbonation of $\text{Mg}(\text{OH})_2$ at $300\text{ }^\circ\text{C}$. The reaction mechanism proposed in this report might not be necessarily valid for the reactions occurring at higher temperature than $300\text{ }^\circ\text{C}$. Carbonation reactions of $\text{Mg}(\text{OH})_2$ by others were carried out typically around $500\text{ }^\circ\text{C}$. At higher temperature, reaction mechanism almost certainly should get much more complex, because all those reactions and changes, such as dehydroxylation, carbonation, decarbonation, translamellar cleavage, and thickening of product layer, would progress simultaneously. Still, the observations made in this study give a very important glimpse into such complex process. Apparently, the carbonation reaction was occurring on the surface of in-situ generated defective MgO , rather than through direct reaction with $\text{Mg}(\text{OH})_2$. Therefore, the carbonation of $\text{Mg}(\text{OH})_2$ does not appear to proceed *via* reaction (3) above. Instead, it can be rewritten as followings. MgO^* designates highly reactive MgO which contains high concentration of defective sites.



With MgO^* involved, thermodynamic parameters for the

above reactions cannot be known accurately without carefully designed experiments. But, it is interesting to note that reaction (6) actually occur at 300 °C, in dynamic condition. Calorimetric study on MgO with high surface area showed that the standard heat of formation for MgO* is substantially higher than bulk MgO.²⁹ The study was carried out only up to 100 m²/g BET surface area. An intriguing curiosity arises on the outcome if the size of the MgO* particles gets very small while raising surface area further in large extent. We are on further pursuing for the answer to this intriguing question.

References

1. Halmann, M.; Steinberg, M. *Greenhouse Gas Carbon Dioxide Mitigation, Science and Technology*; Lewis Publications: London, U. K., 1999.
2. Lackner, K. S.; Wendt, C. H.; Butt, D. P.; Joyce, E. L., Jr.; Sharp, D. H. *Energy* **1995**, *20*(11), 1153.
3. Butt, D. P.; Lackner, K. S.; Wendt, C. H.; Conzone, S. D.; Kung, H.; Lu, Y.; Bremser, J. K. *J. Amer. Ceram. Soc.* **1996**, *79*(7), 1892.
4. Béarat, H.; McKelvy, M. J.; Chizmeshya, A. V. G.; Sharma, R.; Carpenter, R. W. *J. Amer. Ceram. Soc.* **2002**, *85*(4), 742.
5. Moodie, A. F.; Warble, C. E. *J. Cryst. Growth* **1986**, *74*, 89.
6. Naono, H. *Colloids Surf.* **1989**, *37*, 55.
7. McKelvy, M. J.; Sharma, R.; Chizmeshya, A. V. G.; Carpenter, R. W.; Streib, K. *Chem. Mater.* **2001**, *13*, 921.
8. Gillan, M. J.; Kantorovich, L. N.; Lindan, P. J. D. *Current Opinion in Solid State & Materials Science* **1996**, *1*, 820.
9. Gregg, S. J.; Razouk, R. I. *J. Chem. Soc.* **1949**, S36.
10. Garn, P. D.; Freund, F. *Trans. J. Brit. Ceram. Soc.* **1975**, *74*(1), 23.
11. Evans, J. V.; Whateley, T. L. *Trans. Faraday Soc.* **1967**, *63*, 2769.
12. Fukunda, Y.; Tanabe, K. *Bull. Chem. Soc. Jpn* **1973**, *46*, 1616.
13. Stark, J. V.; Park, D. G.; Lagadic, I.; Klabunde, K. J. *Chem. Mater.* **1996**, *8*, 1904.
14. Philipp, R.; Omata, K.; Aoki, A.; Fujimoto, K. *J. Catal.* **1992**, *134*, 422.
15. Philipp, R.; Fujimoto, K. *J. Phys. Chem.* **1992**, *96*, 9035.
16. Pacchioni, G. *Surf. Sci.* **1993**, *281*, 207.
17. Lee, M. H.; Park, D. G. *Bull. Korean Chem. Soc.* **2003**, *24*(10), 1437.
18. Itoh, H.; Utamapanya, S.; Stark, J. V.; Klabunde, K. J.; Schlup, J. R. *Chem. Mater.* **1993**, *5*, 71.
19. Koper, O. B.; Lagadic, I.; Volodin, A.; Klabunde, K. J. *Chem. Mater.* **1997**, *9*, 2468.
20. Anderson, P. J.; Horlock, R. F.; Oliver, J. F. *Trans. Faraday Soc.* **1965**, *61*, 2754.
21. Coluccia, S.; Marchese, L.; Lavagnino, S.; Anpo, M. *Spectrochim. Acta A* **1987**, *43*(12), 1573.
22. Knözinger, E.; Jacob, K.; Singh, S.; Hofmann, P. *Surf. Sci.* **1993**, *290*, 388.
23. Tsyganenko, A. A.; Filimonov, V. N. *J. Mol. Struct.* **1973**, *19*, 579.
24. Smirnov, E. P.; Tsyganenko, A. A. *Reac. Kinet. Catal. Lett.* **1984**, *26*(3-4), 405.
25. Takezawa, N. *Bull. Chem. Soc. Jpn* **1971**, *44*, 3177.
26. Jones, C. F.; Reeve, R. A.; Rigg, R.; Segall, R. L.; Smart, R. C.; Turner, P. R. *J. Chem. Soc., Faraday Trans. 1* **1984**, *80*, 2609.
27. Lavalley, J. C.; Bensitel, M.; Gallas, J. P.; Lamotter, J.; Busca, G.; Lorenzelli, V. *J. Mol. Struct.* **1988**, *175*, 453.
28. Shido, T.; Asakura, K.; Iwasawa, Y. *J. Chem. Soc., Faraday Trans. 1* **1989**, *85*(2), 441.
29. Beruto, D.; Rossi, P. F.; Searcy, A. W. *J. Phys. Chem.* **1985**, *89*, 1695.